Letters

Anomalies in the Knoop microhardness anisotropy of crystals

The crystals with the same lattice structure and the same slip systems are thought in general to have the same microhardness anisotropy [1, 2]. However an anomalous behaviour is revealed in one group of the cubic crystals with NaCl lattice [3, 4]. The further research of this phenomenon and its origin is very important for understanding the physical nature of microhardness.

The purpose of the present paper is to study the effect of crystal hardness on the Knoop microhardness anisotropy. The investigations were performed on the (0 0 1) planes of KCl, NaCl, LiF, and MgO crystals. The microhardness H was measured for two orientations of the indentor: (1) the long diagonal of the Knoop impression $d \parallel [1\,0\,0]$ and (2) $d \parallel [1\,1\,0]$. Thus obtained values are listed in Table I (P is the load applied to the indentor).

It is seen from the table that the sign of anisotropy is dependent on the hardness of the crystals. The soft crystals KCl and NaCl have $\Delta H>0$ (the microhardness for the first orientation is larger than that for the second one); conversely the hard crystals LiF and MgO have $\Delta H<0$. In this case the anisotropy changes quite regularly in the series of KCl–NaCl–LiF–MgO crystals. Thus in passing from a soft KCl crystal to a harder NaCl crystal the anisotropy of microhardness decreases. It changes sign when further increase in hardness takes place (LiF), but its value is rather small. Marked anisotropy is observed in going from LiF to the hardest MgO crystal. The findings for LiF and MgO crystals are similar to the results of Brookes *et al.* [1] and for KCl crystals are analogous to the data of [3]. The change of the sign of microhardness anistropy due to hardening in the series KCl–NaCl–LiF–MgO correlates well with the results obtained in investigating indentation creep in crystals with the rock salt structure [4]. Thus it was observed in [4] that the hardening of NaCl crystals caused by lowering of the temperature follows the relation $H_{[1\,0\,0]}<H_{[1\,1\,0]}$; the softening (lowering of

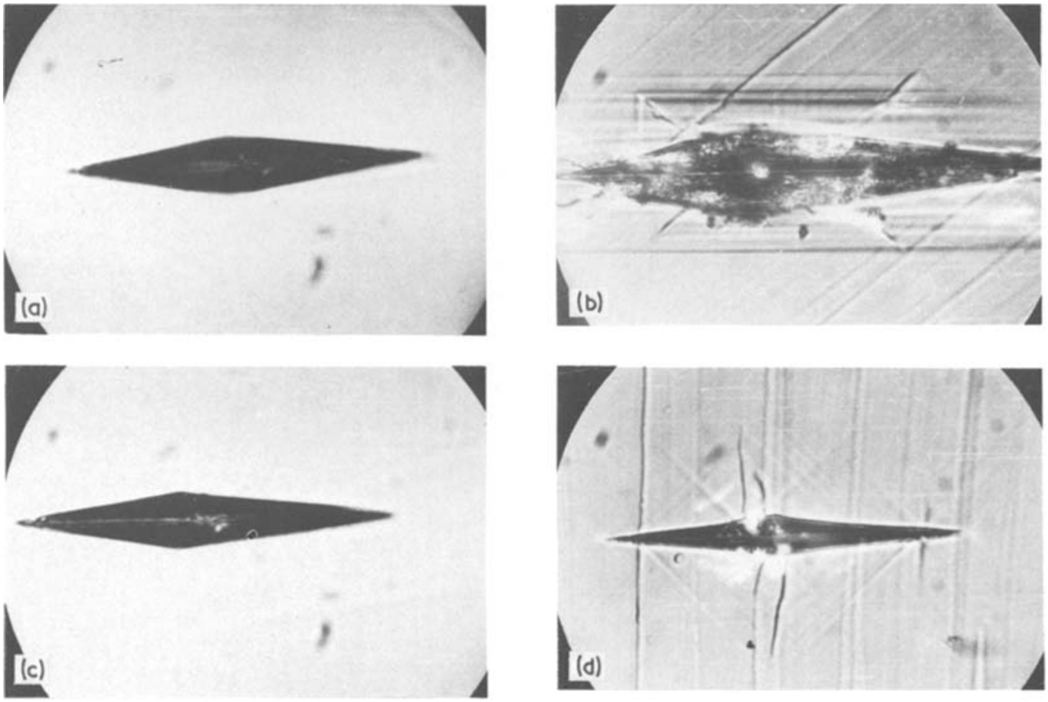

Figure 1 Shape of the indentations on the (0 0 1) plane of KCl (a, c) and MgO (b, d) crystals in two indentor orientations. (a, b) $d \parallel [1\,0\,0]$; (c, d) $d \parallel [1\,1\,0]$. (a, c) $P = 5$ g; (b, d) $P = 400$ g (× 450).

TABLE I

Crystal	P(g)	$H_{[100]}$ (kg mm^{-2})	$H_{[110]}$ (kg mm^{-2})	$\Delta H = H_{[100]} - H_{[110]}$ (kg mm^{-2})	$\lvert\Delta H\rvert/H_{[100]}$ (%)
KCl	10	9.7 ± 0.1	8.3 ± 0.1	1.4	14.4
NaCl	20	20.1 ± 0.2	19.5 ± 0.6	0.6	3.0
LiF	20	108 ± 2.2	114 ± 2.0	− 6	5.5
MgO	100	430 ± 10	840 ± 32	−410	95.3

TABLE II

Irradiation time (h)	H(kg mm^{-2})		$\Delta H = H_{[100]} - H_{[110]}$ (kg mm^{-2})	$\Delta H/H_{[100]}$ (%)
	$d \parallel [1\,0\,0]$	$d \parallel 1\,1\,0]$		
0	20.2 ± 0.2	18.7 ± 0.2	1.5	7.3
2	23.4 ± 0.3	21.5 ± 0.3	1.9	8.1
5	28.2 ± 0.7	26.6 ± 0.7	1.6	9.7
15	33.0 ± 1.5	30.0 ± 0.1	2.6	7.9

microhardness) of MgO crystals with increase of temperature and indentation time corresponds to the anisotropy of microhardness $H_{[100]} > H_{[110]}$, which is unusual for these crystals.

The results obtained in the present paper are clearly illustrated in Fig. 1.

It is known that exposure to ionizing radiation results in an increase of crystal hardness [2, 5–7]. Therefore X-irradiation of NaCl crystals was performed to see whether the irradiation-hardening influenced the magnitude and character of the microhardness anisotropy. The samples were irradiated by soft X-rays; a copper target operated at 30 kV and 4 mA was used; the crystals were placed immediately before the window of the X-ray tube. The results obtained in these experiments are listed in Table II.

It follows from the table that the irradiation results in an increase in microhardness, though it does not affect the microhardness anisotropy. The radiation values seem to be insufficient to change the sign of the anisotropy. It is likely that this result is connected with the fact that the nature of radiation hardening is different from the nature of hardening in the series of crystals KCl–NaCl–LiF–MgO or the nature of temperature hardening.

The interpretation of the anisotropy of Knoop microhardness on single crystal facets is usually based on the effective resolved shear stress model [1, 8]. However this explanation is unsuitable for the results obtained in the present paper (Table I): Crystals having the same slip systems show a different anisotropy of Knoop microhardness.

In the (0 0 1) plane of alkali halide crystals it is shown [2] that the dependence of Vickers microhardness on the indentor orientation is significantly affected by the hills of pressed-out material. However topographical investigations with an interference microscope showed that the surface near the ends of the long diagonal of the Knoop impression (this diagonal is measured for

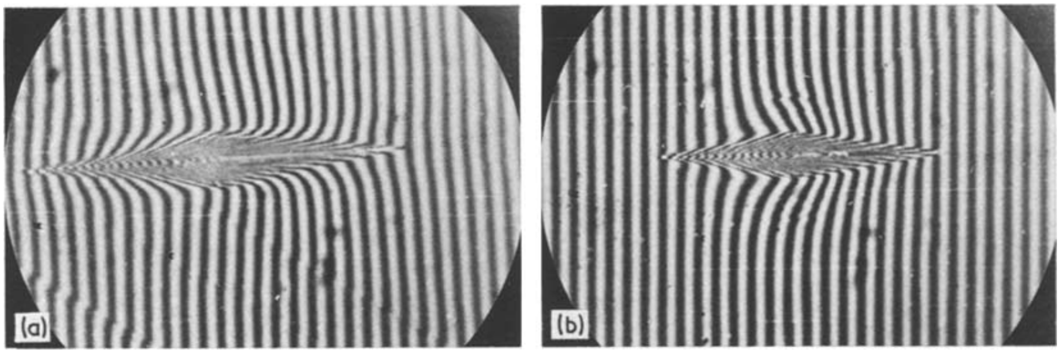

Figure 2 Interferograms of the surface near the indentations on the (0 0 1) plane of (a) unirradiated and (b) irradiated NaCl crystals. $d \parallel [1\,0\,0]$, $P = 10$ g (× 450).

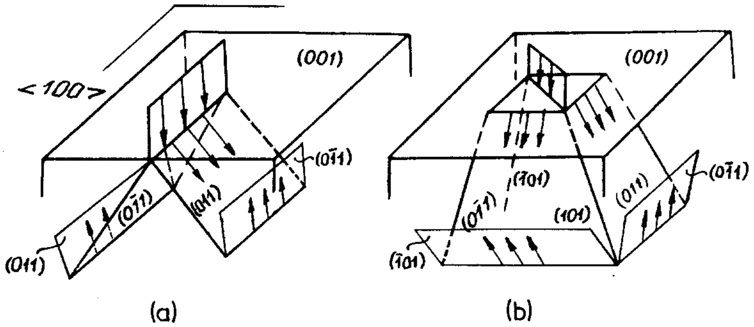

Figure 3 Arrangement of the most active $\{110\}_{45}$ slip planes in the indentation of the knife aligned in the (a) [1 0 0] and (b) [1 1 0] directions.

the calculation of Knoop microhardness values) was practically flat (Fig. 2). Both the unirradiated and irradiated crystals exhibited this property. The latter samples have usually fairly marked hills of pressed-out material. The observation of the surface relief near the end of the short diagonal of the impression (Fig. 2) demonstrates this fact. Now one can conclude that Knoop microhardness anisotropy is not affected by the hills of the material.

The following considerations may have a bearing on the nature of the anomalous microhardness anisotropy. As was previously shown [2, 9], the preferential plastic flow had occurred on $\{110\}_{45}$ slip planes (these planes intersect the (0 0 1) surface with inclination 45°) in indentation on the cube face of alkali halide crystals (Vickers diamond, cone, sphere, knife were used for these experiments). The model of plastic flow in such an indentation was suggested [2]. This model is in agreement with experiment and it may be used for the interpretation of some representative features of plastic deformation.

The stress distribution arising in the crystal in Knoop diamond indentation is similar to that observed for the knife indentor. The main slip planes which were active during plastic deformation in the latter case have been found (Fig. 3) [2].

This result, combined with the model of plastic flow, may allow the following property of Knoop indentation to be assumed. When the long diagonal of the indentation is parallel to [1 0 0] the deformation develops due to intensive slip on two $\{110\}_{45}$ planes –(0 1 1) and $(0\bar{1}1)$ (Fig. 3a). The other indentor orientation ($d \parallel [110]$) causes the deformation of four equivalent $\{110\}_{45}$ planes to be developed (Fig. 3b), but the slip is less intensive than compared with the previous case.

The study of the surface relief in the vicinity of the indentation confirms this assumption. The clear-cut example of that difference appears to be the pattern of slip lines around the indentations of MgO crystals. Thus the intensive slip bands are seen near the indentation shown in Fig. 1b; These bands are the (0 1 1) and $(0\bar{1}1)$ traces on the (0 0 1) plane. The topographical (Fig. 4) investigation shows the surface rise in these regions. It confirms that upward material movements in indentation occur according to the model of Fig. 3a.

The slip lines of the four $\{110\}_{45}$ systems

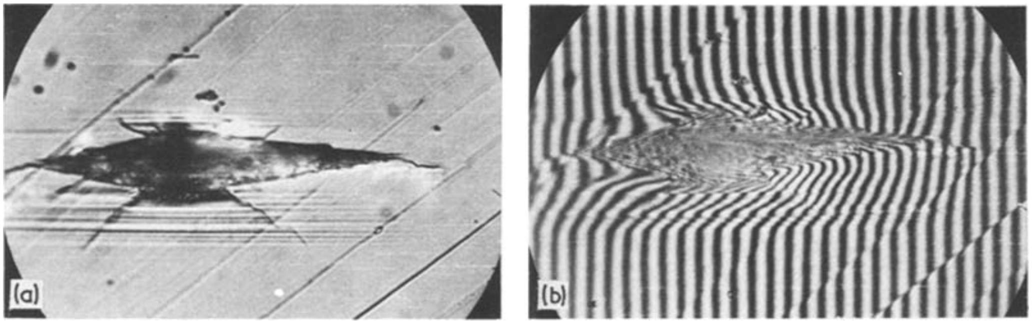

Figure 4 Shape of the indentation (a) and its interferogram (b) on the (0 0 1) plane of MgO. $P = 200$ g, $d \parallel [100]$ (X 450).

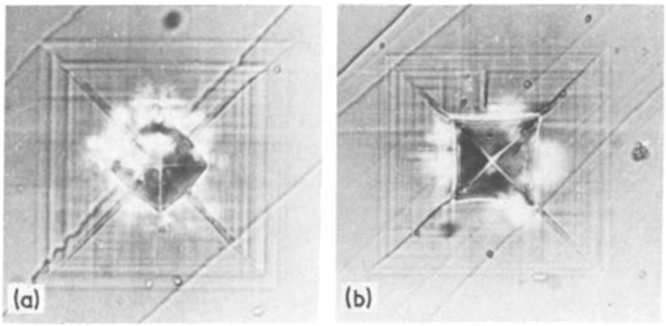

Figure 5 Shape of the indentations on the (0 0 1) plane of MgO in indentation of Vickers diamond. (a) $d \parallel [1\,0\,0]$, (b) $d \parallel [1\,1\,0]$. $P = 200$ g (× 580).

really appear near the indentation of second orientation (Fig. 1b), but these lines are less strongly marked than in the previous case. Thus favourable conditions for intensive glide on the $\{1\,1\,0\}_{45}$ planes arise when $d \parallel [1\,0\,0]$. However the stress distribution causes the deformation on these planes to be hindered when $d \parallel [1\,1\,0]$. As the indentation process on the (0 0 1) plane is controlled by a slip system $\{1\,1\,0\}_{45}$ one can observe that the indentation size is larger in the case of the first orientation than for the second one.

This explanation is true for the hard crystals. It rests on the analysis of the mutual arrangement of the indentor and the slip planes and does not take into account such factors as cross-glide, and work-hardening.

If the slip near the surface of a hard crystal occurs on the (0 1 1) and $(0\,\bar{1}\,1)$ planes (orientation $d \parallel [1\,0\,0]$) then it can easily continue on these planes within the crystal and also upward material movements take place rather easily. In soft crystals an intensive cross-glide causes the appearance of more complicated dislocation structures than in the previous case and a stronger work-hardening is observed. Therefore the deformation on the (0 1 1) and $(0\,\bar{1}\,1)$ planes is hindered and no sufficient stresses arise on the other two $\{1\,1\,0\}_{45}$ planes.

Unlike the $d \parallel [1\,0\,0]$ orientation the development of the deformation on the four equivalent $\{1\,1\,0\}_{45}$ planes occurs in the case of the $d \parallel [1\,1\,0]$ orientation, and for soft crystals it may be more favourable than the initial intensive extension of the deformation only on two planes.

This explanation of the change of the sign of microhardness anisotropy in passing from hard crystals to the soft ones may be regarded only as an assumption. Further work is necessary to clear up this problem. It is interesting to note that the observations of the dislocation structures resulting from the indentation confirm this assumption.

Let us compare the results obtained in the present paper with the data for the microhardness anisotropy in the case of Vickers diamond. Both our investigations performed on the (0 0 1) planes of KCl, NaCl, LiF, MgO (D.S. Pishkova took part in these experiments) and literature data [10] indicate that all the crystals have the same anisotropy of microhardness (maximum microhardness when $d \parallel \langle 1\,0\,0 \rangle$ and minimum microhardness when $d \parallel \langle 1\,1\,0 \rangle$). It must be concluded from this that microhardness anisotropy of LiF and MgO is contrary to that observed in Knoop indentation (Table I).

One can explain this curious fact as follows: (1) Vickers microhardness anisotropy is significantly affected by the hills of pressed-out material; (2) the slip on the four $\{1\,1\,0\}_{45}$ planes takes place for the both indentor orientations but it is more intensive when $d \parallel \langle 1\,1\,0 \rangle$ (it corresponds with the Knoop indentor orientation $d \parallel \langle 1\,0\,0 \rangle$, as opposed to the case of the Knoop indentor, the sides of Vickers indentation are at 45° to the diagonals). Therefore the indentation size is larger for this orientation than for the other one. It can be clearly seen on the (0 0 1) plane of MgO crystals (Fig. 5).

References

1. C. A. BROOKES, J. B. O'NEILL and B. A. REDFERN, *Proc. Roy. Soc. Lond.* **A322** (1971) 73.
2. Yu. S. BOYARSKAYA "Deformation of crystals in microhardness testing" (Stiintza. Kishinev, 1972).

3. C. Y. CHIN, L. G. VAN UITERT, M. L. GREEN and G. ZYDZIK, *Scripta Met.* **6** (1972) 503.
4. C. A. BROOKES, R. P. BURNAND and J. E. MORGAN, *J. Mater. Sci.* **10** (1975) 2171.
5. E. AERTS, S. AMELINCKX and W. DEKEYSER, *Acta Met.* **7** (1959) 29.
6. W. H. VAUGHAN and J. W. DAVISSON, *ibid.* **6** (1958) 554.
7. M. PERINOVÁ and A. A. URUSOVSKAIA, *Czechoslov. J. Phys.* **B16** (1966) 791.
8. D. N. FRENCH and D. A. THOMAS, *Trans Met. Sco. AIME* **233** (1965) 950.
9. M. V. SWAIN and B. R. LAWN, *Phys. Stat. Sol.* **35** (1969) 909.
10. E. S. BERKOVICH, *Zavodskaya Laboratoriya* **10** (1963) 1250.

Received 28 February
and accepted 7 June 1978

Yu. S. BOYARSKAYA
D. Z. GRABKO
E. I. PURICH
Institute of Applied Physics,
Moldavian Academy of Sciences,
Kishinev-28, USSR

On creep ductility of two dilute zinc alloys

The effect of small additions of Al and Cu on slow strain-rate tensile ductility of Zn at elevated temperatures are reported. Two dilute alloys, high purity Zn (99.99% pure) with addition of 0.16 at.% Al (Alloy A) or 0.14 at.% Cu (Alloy C) have been examined. The study assumes significance in view of the fact that Al is a solute in Zn with a distribution coefficient K less than 1 (about 0.25) while for the Cu solute, K is greater than 1. The work of Aust *et al.* [1] has shown that Al atoms experience attractive interactions with grain boundaries in polycrystalline Zn, tend to get adsorbed at the grain boundaries and cause grain-boundary hardening. On the other hand, Cu atoms experience repulsive interactions, stay away from grain boundaries in Zn and give rise to grain-boundary softening. Our interest was to investigate the effect of this distinct difference in solute distribution on the creep ductility of Zn.

Standard Hounsfield tensile specimens of gauge diameter 4.7 mm and gauge length 16 mm were machined from extruded rods of 10 mm diameter in each case. The specimens were chemically polished in a solution containing 32 g chromic acid and 4 g sodium sulphate in 100 ml water to remove the deformed layer. The polished specimens were annealed at 250° C for 1 h to yield average intercept grain sizes of 80 and 120 μm in Alloys A and C respectively. The specimens were tested in tension at 23° C (0.41 T_m, where T_m is the melting temperature in degree Kelvin), 67° C (0.49 T_m), 100° C (0.54 T_m), 150° C (0.61 T_m) and 200° C (0.68 T_m) on a modified Hounsfield tensometer [2] at a nominal strain-rate of 3×10^6 sec^{-1}. The fractured specimens were rapidly cooled by a jet of cold air in order to retain the microstructure developed at the test temperature. The tested specimens were longitudinally sectioned and polished for metallography. The extent of creep cavitation in the fractured samples was assessed by estimating the percent volume fraction (f) of cavities, using the formula [3]:

$$f = \frac{8}{3\pi} \cdot \frac{N_L^2}{N_A} \times 100 \qquad (1)$$

where N_L and N_A are respectively the number of cavities per unit length and unit area. Measurements of N_L and N_A were made at × 200 magnification and the entire area covering the gauge length of the samples was scanned for the purpose.

The variation with test temperature of percent elongation at fracture of the two alloys is shown in Fig. 1. The ductility of alloy C remains more or less the same over the entire temperature range. On the other hand, the ductility of alloy A increases sharply at temperatures above 67° C, attains a maximum value at 150° C and then again decreases to a lower value at 200° C. At any test temperature the ductility of Alloy A is higher than that of Alloy C and at 150° C Alloy A exhibits three times as large a percentage elongation as observed in Alloy C. There is some difference in the grain sizes of the above two alloys as mentioned above (see also Fig. 2) but the vast difference in ductility cannot be attributed to difference in grain size alone. Furthermore, similar ductility differences in these two alloys have been observed by Roth *et al.* [4] who tested specimens of equal grain sizes of these alloys. We shall